Inorganic Chemistry

pubs.acs.org/IC Article

Diffusion Control in Single-Site Zinc Reticular Amination Catalysts

Francisco G. Cirujano,* Elena López-Maya, Neyvis Almora-Barrios, Ana Rubio-Gaspar, Nuria Martín, Jorge A. R. Navarro, and Carlos Martí-Gastaldo*

Cite This: https://dx.doi.org/10.1021/acs.inorgchem.0c02624 Read Online

ACCESS | Metrics & More | Article Recommendations | Supporting Information

ABSTRACT: Zn-containing metal−organic frameworks have been used for the first time as heterogeneous catalysts in the amination of C−Cl bonds. The use of extended bis(pyrazolate) linkers can generate highly porous architectures, which favor the diffusion of amines to the confined spaces with respect to other imidazolate frameworks with narrower pore windows. The N_4Zn nodes of the Zn-reticular framework show comparable activity to state-of-the-art homogeneous Zn amination catalysts, avoiding the use of basic conditions, precious metals, or other additives. This is combined with long-term activity and stability upon several reaction cycles, without contamination of the reaction product.

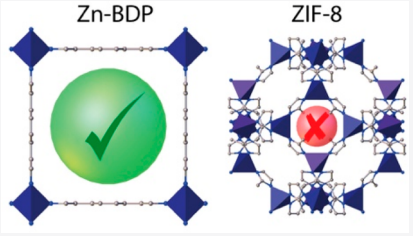

INTRODUCTION

C−N couplings involving the addition of N−H groups to C−Cl bonds in N-heterocycles are important reaction steps during the assembly of high value-added molecules. In the pharmaceutical industry, efficient methods for the production of substituted pyridines by C−Cl amination are urgently needed.[1,2] Contemporary synthetic methods as Buchwald−Hartwig or Ullmann-type C−N couplings often require costly, air-sensitive homogeneous catalysts and stoichiometric amounts of base.[3] In this sense, the use of a zinc(II) Lewis acid (which is cheaper, less toxic, and naturally more abundant than precious metal catalysts) has been reported to activate 4-chloropyridine during nucleophilic aromatic substitutions with amines.[4,5] However, these promising results also anticipate the limitations intrinsic to homogeneous catalysis, as the recovery and recycle of the catalyst or the eventual contamination of the product. In order to improve the sustainability and innovate the catalysis of organic transformations, different approaches such as the use of ionic liquids, nanocages, coordination networks, or metal−organic frameworks (MOFs) are bridging the gap between traditional homogeneous and heterogeneous catalysts.[6−14] The incorporation of Zn(II) as a single site (well-positioned and separated) in open frameworks as zeolites, coordination polymers, or MOFs would permit translating this reactivity to the heterogeneous phase for simple separation of the product, thus avoiding its contamination.[15−21]

Pioneering studies of copper active sites in MOFs for N-arylations of aryl bromides with aromatic amines and N-heterocycles using Ullmann-type couplings have been reported.[22,23] However, the harsh conditions used, which include large amounts of base, compromises the stability and recyclability of the framework. This limitation might be more easily overcome by using earth abundant metal-azolate frameworks based on extended linkers.[24−28] This family of robust MOFs have demonstrated catalytic activity in aldol condensations−Michael-type additions,[29] hydroaminations,[30] cross-couplings,[31,32] and carboxylations.[33] Pyrazolate groups favor soft−soft acid−base interactions (with divalent metals) for higher thermal stability and exceptional chemical stability in acid and basic conditions, compared to carboxylate MOFs.[22] Moreover, only one Zn single site is present at the N_4Zn SBUs of the azolate-type Zn-MOFs (see Figure 1), with respect to the four Zn present as $Zn_4O(CO_2)_3$ in carboxylate-type Zn-MOFs (e.g., MOF-5, MOF-74). However, the use of parent MBDP frameworks (BDP = 1,4-bis(pyrazol-4-yl)benzene) as catalysts has been largely overlooked.[34,35] Previous works rely on the encapsulation of metals (Cu, Pd, Ag) in the pores of the

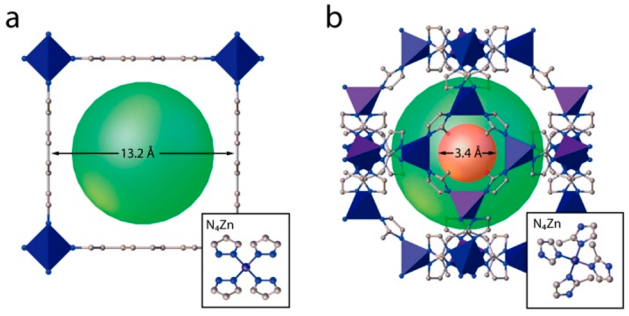

Figure 1. Structure of the N_4Zn nodes in ZnBDP (a) and ZIF-8 (b). The green spheres represent the pore diameter of similar size in both cases. Dimensions of the pore aperture are indicated and highlighted with a red sphere in the case of ZIF-8 to account for disfavored substrate diffusion.

Received: September 2, 2020

framework, which are responsible for the catalytic activity, while the framework is exclusively used as innocent porous support to prevent the aggregation and deactivation of active sites.

Here we study for the first time the activity of unmodified ZnBDP as a heterogeneous catalyst, based on the reported $Zn(NO_3)_2$ homogeneous C−Cl amination catalyst.[4] This framework consists of tetrahedrally coordinated N_4Zn metal centers interconnected by BDP linkers to generate 3D square channels with edges of 13.2 Å, large pores of close to 11.1 Å (see Figure 1a).[36−38] In order to account for the changes of porosity over substrate diffusion and performance, the zinc-pyrazolate ZnBDP was compared with that of zinc-imidazolate ZIF-8. This choice is based on the similar environment of the ZnN_4 units, but featuring a different porous architecture with large 11.6 Å pores connected through small apertures of 3.4 Å (see Figure 1b).[39]

RESULTS AND DISCUSSION

We tested both Zn reticular catalysts in the proof-of-concept amination of the sp^2 C4 carbon of 4-chloropyridine (Cl-py) with morpholine. The yield of the 4-aminated pyridine product after 72 h of reaction increases in the order ZIF-8 (26%) < ZnBDP (51%) < $Zn(NO_3)_2$ (82%), for the same catalyst mass (see Figure 2a). The kinetic rate constants were obtained from

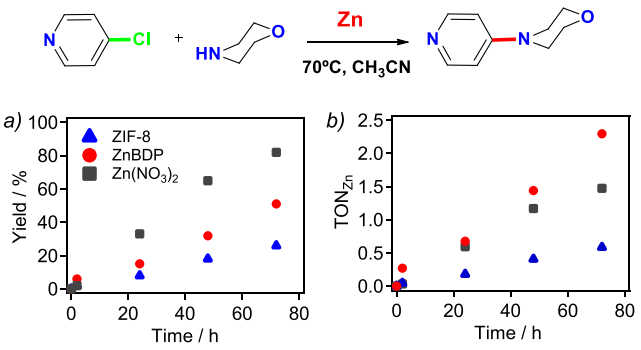

Figure 2. Kinetic profiles (a) and activity (TON_{Zn}) expressed in mol of Cl-py converted divided per mol of Zn (b), for the amination of 10 mg of Cl-py catalyzed by 10 mg of ZnBDP (red) or ZIF-8 (blue) with respect to $Zn(NO_3)_2$ (black).

the linear fit of the logarithm of the 4-chloropyridine conversion vs time, assuming a pseudo-first-order reaction, which resulted in different slopes (see Figure S5 in the Supporting Information). The kinetic rate constant increases as $k_{ZIF\text{-}8}$ (0.004 h^{-1}) < k_{ZnBDP} (0.009 h^{-1}) < k_{ZnNO3} (0.024 h^{-1}). For the same Zn-catalyst mass, the Cl-py/Zn molar ratio increases in the order $Zn(NO_3)_2$ < ZIF-8 < ZnBDP (being 1.8 < 2.3 < 4.5, respectively). When the kinetic rate constants are multiplied by the corresponding substrate/catalyst ratio, a normalized rate constant per Zn active site is obtained. Its value is similar for the heterogeneous ZnBDP and the homogeneous $Zn(NO_3)_2$ (ca. 0.04 h^{-1}) and four times higher than in the case of microporous ZIF-8 (ca. 0.01 h^{-1}).

The number of product molecules per zinc site (TON_{Zn}) during the course of the reaction is represented in Figure 2b. It indicates the good catalytic performance of ZnBDP with respect to ZIF-8 and the $Zn(NO_3)_2$ homogeneous catalyst.[4] In contrast to the soluble Zn^{2+} species, which are not possible to recover and recycle, ZnBDP can be isolated by simple centrifugation and employed in subsequent reaction cycles without apparent loss in activity: k_{ZnBDP} = 9.3 × 10^{-3}, 8.8 × 10^{-3}, 8.2 × 10^{-3}, and 7.8 × 10^{-3} h^{-1} for the four subsequent cycles (see Figure S6 in the Supporting Information). Therefore, the cumulative rate constant per Zn active site after three cycles is 3.8 times higher when using the ZnBDP MOF (0.15 h^{-1}) with respect to the homogeneous $Zn(NO_3)_2$ catalyst (0.04 h^{-1}). The high stability of both MOFs is proven due to the maintenance of XRD patterns after 72 h of reaction, with only minor changes attributed to changes in pore occupancy (see Figure 3).[38] A hot filtration test of ZnBDP

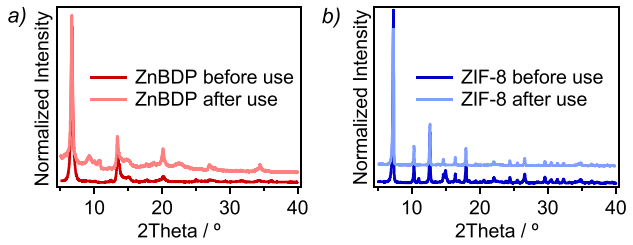

Figure 3. Powder XRD patters of ZnBDP (a) with respect to ZIF-8 (b) catalysts before and after the amination of Cl-py with morpholine.

demonstrated the heterogeneous nature of the reaction (see Figure S6 in the Supporting Information). ICP analysis of the filtrate results in 0.21 wt % Zn leaching from ZnBDP. Taking into account that 13 wt % of Zn in the MOF structure is used with respect to 4-chloropyridine, only 0.03 wt % Zn will be in the form of leached homogeneous Zn^{2+}. This amount is way below the 1.4 wt % Zn used in the reported homogeneous catalyzed process,[4] confirming the results of the hot filtration tests. Furthermore, no evidence of 4-pyridination of 1,4-bis(pyrazol-4-yl)benzene ligand was found according to the NMR spectra of the digested MOF before and after the reaction (see Figure S7). Therefore, the changes in catalytic performance between single-site Zn(II) frameworks cannot be ascribed to the potential degradation of ZnBDP but to differences imposed by the dimensions of their pores and channels.

To further confirm the key role played by the diffusion of the substrates into the ZnN_4-MOF active sites, solid−liquid adsorption experiments of a solution of 4-chloropyridine (Cl-py) in CH_3CN (2.5 mg·mL^{-1}) were performed. The ZnBDP shows a higher uptake with respect to ZIF-8, resulting in 1.0 vs 0.3 $mol_{Cl\text{-}py}$·mol_{Zn}^{-1} (see Table S4 in the Supporting Information). A computational study has been performed with both reticular Zn catalysts (i.e., $Zn_{12}(C_4N_2H_5)_{24}$ and $Zn_4(C_{12}N_4H_8)_4$ modeled crystalline cells of ZIF-8 and ZnBDP, respectively) in order to understand the experimental results. The calculated values are in line with the experimental uptake of Cl-py molecules by the MOFs, corresponding to 0.4 and 1.0 $mol_{Cl\text{-}py\ or\ morpholine}$·$mol_{Zn}^{-1}$ docked in ZIF-8 and ZnBDP, respectively. More importantly, the molecular dynamics results indicate a higher diffusivity in the ZnBDP with respect to ZIF-8, especially in the case of the amine nucleophile (2 × 10^{-5} vs 1 × 10^{-7} cm^2·s^{-1}), as shown in Figure 4 (molecule A). The adsorption and diffusion results further confirm that the changes in the pore window of ZnBDP and ZIF-8 may be the origin of their different catalytic performance. On the one hand, the 1.3 nm edges of the square channels from ZnBDP favor the infiltration and docking of Cl-py molecules inside the

https://dx.doi.org/10.1021/acs.inorgchem.0c02624
Inorg. Chem. XXXX, XXX, XXX−XXX

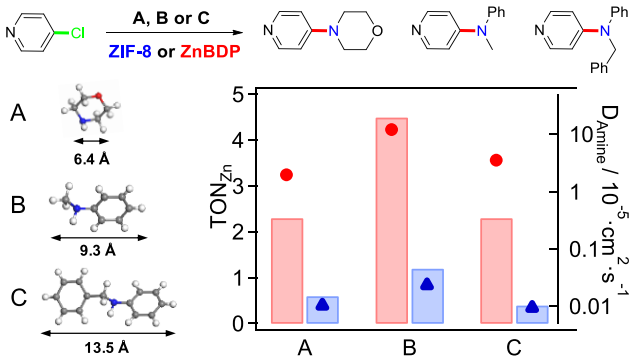

Figure 4. TON of Zn sites (bars, left axis) in the amination of Cl-py with morpholine (A), *N*-methylaniline (B), and *N*-phenylaniline (C), together with the diffusivity (D_{amine}) of A, B, or C (circles and triangles, logarithmic right axis) in ZnBDP (red) or ZIF-8 (blue).

pore cavities for subsequent reaction with morpholine. On the other hand, the restricted diffusion of reactants across the 0.3 nm pore windows of ZIF-8 precludes the inner Zn−N active sites to activate the reactants for the amination reaction (see Figure 1).

To rule out the contribution of the Zn active sites located at the external surface of the crystals, the catalytic activity of a second ZIF-8 sample with a higher external surface area was tested (see ZIF-8_{H_2O} in Figure S1 and Table S1).[40] The yield obtained after 48 h of reaction between Cl-py and amine A is similar with both samples (~20%), confirming the dominant role of the microporous area and how catalytic activity seems to be restricted to the accessibility of the substrates to the pores of the bulk crystal. Therefore, it seems plausible that when using ZnBDP, the rapid diffusion and confinement of the amination substrates inside the large MOF pores favor the course of the reaction, without the diffusion limitations toward the inner active sites occurring in ZIF-8.

Other aryl halides and NH derivatives were employed as substrates of the ZnBDP reticular catalysts. For instance, the reaction of morpholine with 4-chloroquinoline results in a slightly higher yield of the pharmaceutically relevant 4-aminoquinoline,[2] with respect to 4-chloropyridine (25% vs 15% respectively) after 24 h of reaction (see Figure S9). The higher reactivity of the quinoline derivative (having one extra benzene ring) with respect to the pyridine one may be the result of better solubility in the reaction media and more favorable interactions with the aromatic linker of the ZnBDP. Two additional *N*-substituted anilines with different substituent sizes, i.e. *N*-methylaniline (B in Figure 4) and *N*-phenylaniline (C in Figure 4), were employed in the amination of Cl-py, in order to check the effect of the substituent size (methyl vs phenyl) on the catalytic performance of both Zn-reticular catalysts. The yields of the two new 4-aminopyridines obtained after 72 h with ZnBDP as catalyst were 98% and 50% for amine B and C, respectively. However, these yields decreased to 51% and 17% (for B and C, respectively) when using ZIF-8 as catalyst (see Table S3).

The higher TON_{ZnBDP}/TON_{ZIF-8} ratio when using amine C as the amination agent with respect to amine B (TON_{ZnBDP}/TON_{ZIF-8} = 5.8 vs 3.8) suggests the steric hindrance of the phenyl substituted amine when diffusing into the MOF pores. Thus, despite the similar difference in activity between ZnBDP and ZIF-8 in the case of small *N*-methylaniline (ca. 0.9 nm size), the performance of ZnBDP is boosted with respect to ZIF-8 in the case of bulkier substrates such as *N*-phenylaniline (ca. 1.3 nm size). Indeed, molecular mechanics simulations confirm the docking of 6 and 3 molecules of *N*-methylaniline, or 3 and 1 molecules of *N*-phenylaniline for ZnBDP and ZIF-8, respectively (see Figures S10−S13 in the Supporting Information). As previously described for morpholine, the diffusivity of both reaction substrates is higher on ZnBDP than in ZIF-8 (see Table S5). The changes are more pronounced when passing from amine B to amine C, where only steric effects are introduced by changing one of the *N*-substituents. The D_{ZnBDP}/D_{ZIF-8} diffusivity ratio in the case of amine B is 522, with respect to the value of 376 for amine C. In both cases, the diffusivity of the amine in the large pores of ZnBDP is up to 3 orders of magnitude higher with respect to the traditional ZIF-8 Zn reticular catalyst.

Furthermore, density functional theory (DFT, see Supporting Information for details) allows us to propose a reaction mechanism based on Zn single sites instead of dual metal sites reported with other MOF catalysts.[41] As shown in Figure 5, the

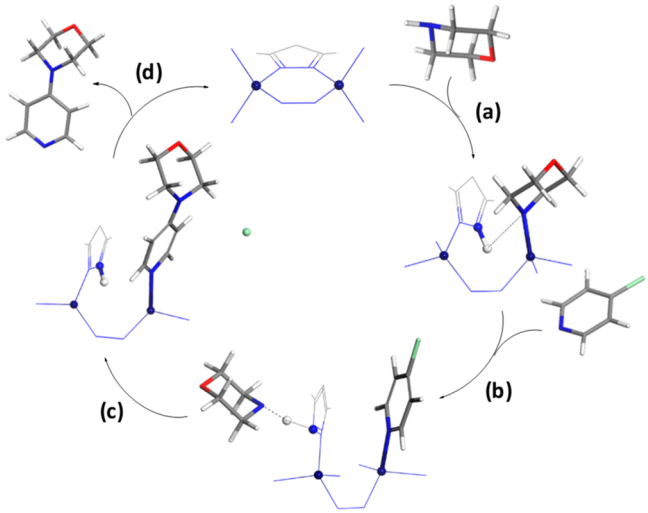

Figure 5. Proposed mechanism for the amination of Cl-py with morpholine catalyzed by acid−base sites in ZnBDP. (a) Interaction of morpholine molecules with the Zn and H-transfer from the morpholine to the N-linker, (b) 4-chloropyridine adsorption on Zn sites. (c) C−N bond formation between 4-chloropyridine and morpholine and (d) active site regeneration.

interaction of morpholine molecules with the Zn atom takes place through a concerted step (Figure 5a), where the proton of the morpholine is transferred to the ligand leaving a free site in the Zn atoms for its adsorption. Although the adsorption strength of the morpholine is weak (+2.9 kJ mol^{-1}), the protonation process of the BDP pyrazolate linker coordinated to the Zn site (transient BDP decoordination of 1 out of the 4 N−Zn bonds) leaves the possibility that Cl-py interacts strongly with the Zn atom by −135.1 kJ mol^{-1} (Figure 5b). This agrees well with the FT-IR spectrum of ZnBDP after 24 h of reaction between Cl-py and morpholine, which shows a band around 1635 cm^{-1} (different from that of the free 4-chloropyridine at 1490 cm^{-1}),[42] suggesting that the N_4Zn SBUs can act as a Lewis acid. These sites are available for interaction with the nitrogen lone pair of 4-chloropyridine (see Figure S8), as recently described for homogeneous Zn(II) complexes.[43] The (reversible) complex formation between the Zn(II) Lewis acid and pyridine Lewis base through the binding

https://dx.doi.org/10.1021/acs.inorgchem.0c02624
Inorg. Chem. XXXX, XXX, XXX−XXX

of Zn to the pyridine nitrogen has been also proposed for the homogeneous case.[4,5] Finally, the formation of the product after the S_NAr reaction is exothermic by −212.3 kJ mol^{-1} (Figure 5c).

Our simulations suggest that differences in activity are associated with the acid−base properties of the reagents with respect to the linker. This is supported by the fact that the pK_a of the −NH− in the pyrazolate is much higher than that of morpholine (19.8 vs 8.4, respectively). In addition, we have studied an alternative model in which both the morpholine and Cl-py interact with two vicinal Zn atoms (presumably at eventual missing-linker defect sites; see Figure S2 and Table S2). This model is exothermic by −35.7 kJ mol^{-1} but significantly less favorable than the single-site model (−131.1 kJ mol^{-1}; see Supporting Information for details). Moreover, the distance between the C of the Cl-py and the N of the morpholine is 4.43 Å, which hinders the S_NAr reaction (see Figure S14) in the dual-site mechanism, with respect to the single-site proposed here. Further studies for the validation of the proposed mechanism are ongoing.

CONCLUSIONS

In conclusion, Zn-catalyzed amination of 4-chloropyridine is reported here using a heterogeneous catalyst for the first time. The porous architecture of the ZnBDP MOF provides higher uptake capacity and more favorable mass transfer (up to 3 orders of magnitude higher) compared to microporous ZIF-8. The larger Zn-bis(pyrazolate) cavities favor the transport of the substrate molecules inside the ZnBDP pores, where they access the inner active sites, as shown by the calculated diffusivities of the substrates in both MOFs. In contrast, the Zn sites are less accessible to the reagents in the case of ZIF-8, resulting in a decrease of catalytic activity below half of the value of ZnBDP. TON values of the Zn active sites which are up to 6 times higher are obtained in the transformation of bulky substrates (i.e., *N*-phenylaniline), when those catalytic sites are in a more open Zn-azolate structure. These observations confirm the positive effects of the activation of the 4-chloropyridine and different amine substrates inside the porous spaces of ZnBDP, where the inner Zn active sites are more accessible than in the far more popular zeolitic imidazolate frameworks. The use of the heterogeneous Zn-bis(pyrazolate) catalyst is a sustainable alternative to the use of homogeneous Zn salts, which can be outperformed in terms of activity and stability, paving the way for the synthesis of pharmaceutically interesting intermediates in an environmentally benign manner.

ASSOCIATED CONTENT

Supporting Information

The Supporting Information is available free of charge at https://pubs.acs.org/doi/10.1021/acs.inorgchem.0c02624.

Synthesis and characterization of the Zn-MOF catalysts, catalytic and computational details (PDF)

AUTHOR INFORMATION

Corresponding Authors

Francisco G. Cirujano − *Instituto de Ciencia Molecular (ICMol), Universitat de València, 46980 Paterna, Valencia, Spain*; orcid.org/0000-0002-0159-5777; Email: francisco.c.garcia@uv.es

Carlos Martí-Gastaldo − *Instituto de Ciencia Molecular (ICMol), Universitat de València, 46980 Paterna, Valencia, Spain*; orcid.org/0000-0003-3203-0047; Email: carlos.marti@uv.es

Authors

Elena López-Maya − *Instituto de Ciencia Molecular (ICMol), Universitat de València, 46980 Paterna, Valencia, Spain*

Neyvis Almora-Barrios − *Instituto de Ciencia Molecular (ICMol), Universitat de València, 46980 Paterna, Valencia, Spain*; orcid.org/0000-0001-5269-2705

Ana Rubio-Gaspar − *Instituto de Ciencia Molecular (ICMol), Universitat de València, 46980 Paterna, Valencia, Spain*

Nuria Martín − *Instituto de Ciencia Molecular (ICMol), Universitat de València, 46980 Paterna, Valencia, Spain*

Jorge A. R. Navarro − *Department of Inorganic Chemistry, University of Granada, 18071 Granada, Spain*

Complete contact information is available at: https://pubs.acs.org/10.1021/acs.inorgchem.0c02624

Notes

The authors declare no competing financial interest.

ACKNOWLEDGMENTS

The project that gave rise to these results received the support of a fellowship from the "la Caixa" Foundation (ID 100010434). The fellowship code is LCF/BQ/PI19/11690011. E.L.-M. thanks the Spanish government for a Juan de la Cierva Fellowship (FJCI-2017-32956). A.R.G. acknowledges funding from Generalitat Valencia and Fondo Social Europeo. N.M. acknowledges the "Juan de la Cierva formación" fellowship with code FJC2018-035455-I. J.A.R.N. is thankful for CTQ2017-84692-R and EU FEDER funding. We also thank the EU (ERC Stg Chem-fs-MOF 714122) and Spanish government (CTQ2017-83486-P and CEX2019-000919-M). UV-Tirant and UV-LluisVives are acknowledged for the computational resources.

REFERENCES

(1) Fussell, S. J.; Luan, A.; Peach, P.; Scotney, G. A three-step synthesis of 4-(4-iodo-1H-pyrazol-1-yl)piperidine, a key intermediate in the synthesis of Crizotinib. *Tetrahedron Lett.* **2012**, *53*, 948−951.

(2) Natarajan, J. K.; Alumasa, J.; Yearick, K.; Ekoue-Kovi, K. A.; Casabianca, L. B.; de Dios, A. C.; Roepe, P. D.; Wolf, C. Overcoming Drug Resistance to Heme-Targeted Antimalarials by Systematic Side Chain Variation of 7-Chloro-4-aminoquinolines. *J. Med. Chem.* **2008**, *51*, 3466−3479.

(3) Surry, D. S.; Buchwald, S. L. Biaryl phosphane ligands in palladium-catalyzed amination. *Angew. Chem., Int. Ed.* **2008**, *47*, 6338−6361.

(4) Abou-Shehada, S.; Teasdale, M. C.; Bull, S. D.; Wade, C. E.; Williams, J. M. J. Lewis acid activation of pyridines for nucleophilic aromatic substitution and conjugate addition. *ChemSusChem* **2015**, *8*, 1083−1087.

(5) Kinens, A.; Balkaitis, S.; Suna, E. Preparative-Scale Synthesis of Vedejs Chiral DMAP Catalysts. *J. Org. Chem.* **2018**, *83*, 12449−12459.

(6) Cirujano, F. G.; Stalpaert, M.; De Vos, D. E. Ionic liquids vs. microporous solids as reusable reaction media for the catalytic C−H functionalization of indoles with alcohols. *Green Chem.* **2018**, *20*, 2481−2485.

(7) Sheng, K.; Fan, L. M.; Tian, X. F.; Gupta, R. K.; Gao, L.; Tung, C. H.; Sun, D. Temperature-induced Sn(II) supramolecular isomeric frameworks as promising heterogeneous catalysts for cyanosilylation of aldehydes. *Sci. China: Chem.* **2020**, *63*, 182−186.

(8) Liu, Y. N.; Su, H. F.; Li, Y. W.; Liu, Q. Y.; Jagličić, Z.; Wang, W. G.; Tung, C. H.; Sun, D. Space Craft-like Octanuclear Co(II)-Silsesquioxane Nanocages: Synthesis, Structure, Magnetic Properties, Solution Behavior, and Catalytic Activity for Hydroboration of Ketones. *Inorg. Chem.* **2019**, *58*, 4574−4582.
(9) Zhao, M.; Huang, S.; Fu, Q.; Li, W.; Guo, R.; Yao, Q.; Wang, F.; Cui, P.; Tung, C. H.; Sun, D. Ambient Chemical Fixation of CO_2 Using a Robust Ag_{27} Cluster-Based Two-Dimensional Metal−Organic Framework. *Angew. Chem., Int. Ed.* **2020**, *59*, 20031−20036.
(10) Xu, Z.; Han, L. L.; Zhuang, G. L.; Bai, J.; Sun, D. In Situ Construction of Three Anion-Dependent Cu(I) Coordination Networks as Promising Heterogeneous Catalysts for Azide−Alkyne "Click" Reactions. *Inorg. Chem.* **2015**, *54*, 4737−4743.
(11) Cao, C. S.; Xia, S. M.; Song, Z. J.; Xu, H.; Shi, Y.; He, L. N.; Cheng, P.; Zhao, B. Highly Efficient Conversion of Propargylic Amines and CO2 Catalyzed by Noble-Metal-Free [Zn116] Nanocages. *Angew. Chem., Int. Ed.* **2020**, *59*, 8586−8593.
(12) Hou, S. L.; Dong, J.; Jiang, X. L.; Jiao, Z. H.; Zhao, B. A Noble-Metal-Free Metal−Organic Framework (MOF) Catalyst for the Highly Efficient Conversion of CO2 with Propargylic Alcohols. *Angew. Chem., Int. Ed.* **2019**, *58*, 577−581.
(13) Cirujano, F. G. Engineered MOFs and Enzymes for the Synthesis of Active Pharmaceutical Ingredients. *ChemCatChem* **2019**, *11*, 5671−5685.
(14) Martin, N.; Cirujano, F. G. Organic synthesis of high added value molecules with MOF catalysts. *Org. Biomol. Chem.* **2020**, *18*, 8058−8073.
(15) Penzien, J.; Müller, T. E.; Lercher, J. A. Zinc-ion exchanged zeolites for the intramolecular hydroamination of 6-aminohex-1-yne. *Chem. Commun.* **2000**, 1753−1754.
(16) Martin, N.; Dusselier, M.; De Vos, D. E.; Cirujano, F. G. Metal-Organic Framework Derived Metal Oxide Clusters in Porous Aluminosilicates: A Catalyst Design for the Synthesis of Bioactive aza-Heterocycles. *ACS Catal.* **2019**, *9*, 44−48.
(17) Marquez, C.; Cirujano, F. G.; Van Goethem, C.; Vankelecom, I.; De Vos, D.; De Baerdemaeker, T. Tunable Prussian blue analogues for the selective synthesis of propargylamines through A3 coupling. *Catal. Sci. Technol.* **2018**, *8*, 2061−2065.
(18) Marquez, C.; Rivera-Torrente, M.; Paalanen, P. P.; Weckhuysen, B. M.; Cirujano, F. G.; De Vos, D.; De Baerdemaeker, T. Increasing the availability of active sites in Zn-Co double metal cyanides by dispersion onto a SiO2 support. *J. Catal.* **2017**, *354*, 92−99.
(19) Tran, U. P. N.; Le, K. K. A.; Phan, N. T. S. Expanding Applications of Metal−Organic Frameworks: Zeolite Imidazolate Framework ZIF-8 as an Efficient Heterogeneous Catalyst for the Knoevenagel Reaction. *ACS Catal.* **2011**, *1* (2), 120−127.
(20) Roy, S.; George, C. B.; Ratner, M. A. Catalysis by a Zinc-Porphyrin-Based Metal−Organic Framework: From Theory to Computational Design. *J. Phys. Chem. C* **2012**, *116*, 23494−23502.
(21) Phan, N. T.S.; Le, K. K.A.; Phan, T. D. MOF-5 as an efficient heterogeneous catalyst for Friedel−Crafts alkylation reactions. *Appl. Catal., A* **2010**, *382*, 246−253.
(22) Maity, T.; Saha, D.; Koner, S. Aromatic N-Arylations Catalyzed by Copper-Anchored Porous Zinc-Based Metal−Organic Framework under Heterogeneous Conditions. *ChemCatChem* **2014**, *6*, 2373−2383.
(23) Truong, T.; Nguyen, C. V.; Truong, N. T.; Phan, N. T. S. Ligand-free N-arylation of heterocycles using metal−organic framework [Cu(INA)2] as an efficient heterogeneous catalyst. *RSC Adv.* **2015**, *5*, 107547−107556.
(24) Navarro, J. A. R. Impact of Defects on Pyrazolate Based Metal Organic Frameworks. *Isr. J. Chem.* **2018**, *58*, 1112−1118.
(25) Desai, A. V.; Sharma, S.; Let, S.; Ghosh, S. K. N-donor linker based metal-organic frameworks (MOFs): Advancement and prospects as functional materials. *Coord. Chem. Rev.* **2019**, *395*, 146−192.
(26) Padial, N.; Procopio, E.; Montoro, C.; López-Maya, E.; Oltra, J.; Colombo, V.; Maspero, A.; Masciocchi, N.; Galli, S.; Senkovska, I.; Kaskel, S.; Barea, E.; Navarro, J. A. R. Highly Hydrophobic Isoreticular Porous Metal−Organic Frameworks for the Capture of Harmful Volatile Organic Compounds. *Angew. Chem., Int. Ed.* **2013**, *52*, 8290−8294.
(27) Taylor, M.; Runčevski, T.; Oktawiec, J.; Gonzalez, M.; Siegelman, R.; Mason, J.; Ye, J.; Brown, C.; Long, J. Tuning the Adsorption-Induced Phase Change in the Flexible Metal−Organic Framework Co(bdp). *J. Am. Chem. Soc.* **2016**, *138*, 15019−15026.
(28) Lv, X.; Wang, K.; Wang, B.; Su, J.; Zou, X.; Xie, Y.; Li, J.; Zhou, H. A Base-Resistant Metalloporphyrin Metal−Organic Framework for C−H Bond Halogenation. *J. Am. Chem. Soc.* **2017**, *139*, 211−217.
(29) Cirujano, F. G.; Lopez-Maya, E.; Rodriguez-Albelo, M.; Barea, E.; Navarro, J. A. R.; De Vos, D. E. Selective one-pot two-step C-C bond formation using MOFs with mild basicity as heterogeneous catalysts. *ChemCatChem* **2017**, *9*, 4019−4023.
(30) Cirujano, F. G.; Lopez-Maya, E.; Navarro, J. A. R.; De Vos, D. E. Pd (II)−Ni (II) pyrazolate framework as active and recyclable catalyst for the hydroamination of terminal alkynes. *Top. Catal.* **2018**, *61*, 1414−1423.
(31) Augustyniak, A. W.; Sadakiyo, M.; Navarro, J. A. R.; Trzeciak, A. M. Palladium nanoparticles supported on a nickel pyrazolate metal organic framework as a catalyst for Suzuki and carbonylative Suzuki couplings. *Dalton Trans.* **2016**, *45*, 13525−13531.
(32) Tarnowicz-Ligus, S.; Augustyniak, A.; Trzeciak, A. M. Incorporation of PdCl2P2 Complexes in Ni-MOF for Catalyzing Heck Arylation of Functionalized Olefins. *Eur. J. Inorg. Chem.* **2019**, *2019*, 4282−4288.
(33) Yang, H.; Zhang, X.; Zhang, G.; Fei, H. An alkaline-resistant Ag(i)-anchored pyrazolate-based metal−organic framework for chemical fixation of CO2. *Chem. Commun.* **2018**, *54*, 4469−4472.
(34) Timokhin, I.; Pettinari, C.; Marchetti, F.; Pettinari, R.; Condello, F.; Galli, S.; Alegria, E. C. B. A.; Martins, L. M. D. R. S.; Pombeiro, A. J. L. Novel Coordination Polymers with (Pyrazolato)-Based Tectons: Catalytic Activity in the Peroxidative Oxidation of Alcohols and Cyclohexane. *Cryst. Growth Des.* **2015**, *15*, 2303−2317.
(35) Lucarelli, C.; Galli, S.; Maspero, A.; Cimino, A.; Bandinelli, C.; Lolli, A.; Ochoa, J. V.; Vaccari, A.; Cavani, F.; Albonetti, S. Adsorbent−Adsorbate Interactions in the Oxidation of HMF Catalyzed by Ni-Based MOFs: A DRIFT and FT-IR Insight. *J. Phys. Chem. C* **2016**, *120* (28), 15310−15321.
(36) Galli, S.; Masciocchi, N.; Colombo, V.; Maspero, A.; Palmisano, G.; Lopez-Garzon, F. J.; Domingo-García, M.; Fernandez-Morales, I.; Barea, E.; Navarro, J. A. R. Adsorption of Harmful Organic Vapors by Flexible Hydrophobic Bis-pyrazolate Based MOFs. *Chem. Mater.* **2010**, *22*, 1664−1672.
(37) Colombo, V.; Montoro, C.; Maspero, A.; Palmisano, G.; Masciocchi, N.; Galli, S.; Barea, E.; Navarro, J. A. R. Tuning the Adsorption Properties of Isoreticular Pyrazolate-Based Metal−Organic Frameworks through Ligand Modification. *J. Am. Chem. Soc.* **2012**, *134*, 12830−12843.
(38) Rojas, S.; Carmona, F. J.; Maldonado, C. R.; Horcajada, P.; Hidalgo, T.; Serre, C.; Navarro, J. A. R.; Barea, E. Nanoscaled Zinc Pyrazolate Metal−Organic Frameworks as Drug-Delivery Systems. *Inorg. Chem.* **2016**, *55*, 2650−2663.
(39) Park, K. S.; Ni, Z.; Côté, A. P.; Choi, J. Y.; Huang, R.; Uribe-Romo, F. J.; Chae, H. K.; O'Keeffe, M.; Yaghi, O. M. Exceptional chemical and thermal stability of zeolitic imidazolate frameworks. *Proc. Natl. Acad. Sci. U. S. A.* **2006**, *103*, 10186−10191.
(40) He, M.; Yao, J.; Liu, Q.; Wang, K.; Chen, F.; Wang, H. Facile synthesis of zeolitic imidazolate framework-8 from a concentrated aqueous solution. *Microporous Mesoporous Mater.* **2014**, *184*, 55−60.
(41) Castells-Gil, J.; Padial, N. M.; Almora-Barrios, N.; Gil-San-Millán, R.; Romero-Ángel, M.; Torres, V.; da Silva, I.; Vieira, B. C. J.; Waerenborgh, J. C.; Jagiello, J.; Navarro, J. A. R.; Tatay, S.; Martí-Gastaldo, C. Heterometallic Titanium-Organic Frameworks as Dual-Metal Catalysts for Synergistic Non-buffered Hydrolysis of Nerve Agent Simulants. *Chem.* **2020**, *6*, 3118.
(42) Busto, E.; Gotor-Fernández, V.; Gotor, V. Enantioselective Synthesis of 4-(Dimethylamino)pyridines through a Chemical

https://dx.doi.org/10.1021/acs.inorgchem.0c02624
Inorg. Chem. XXXX, XXX, XXX−XXX

Oxidation-Enzymatic Reduction Sequence. Application in Asymmetric Catalysis. *Adv. Synth. Catal.* **2006**, *348*, 2626−2632.
(43) Saygili, Y.; Kim, H. S.; Yang, B.; Suo, J.; Muñoz-Garcia, A. B.; Pavone, M.; Hagfeldt, A. Revealing the Mechanism of Doping of spiroMeOTAD via Zn Complexation in the Absence of Oxygen and Light. *ACS Energy Lett.* **2020**, *5*, 1271−1277.

https://dx.doi.org/10.1021/acs.inorgchem.0c02624
Inorg. Chem. XXXX, XXX, XXX−XXX